Supplement of The Cryosphere, 17, 233–253, 2023
https://doi.org/10.5194/tc-17-233-2023-supplement

The Cryosphere Open Access EGU

Supplement of

Causes and evolution of winter polynyas north of Greenland

Younjoo J. Lee et al.

Correspondence to: Younjoo J. Lee (ylee1@nps.edu)

Table S1. One-way ANOVA test of the geopotential height (m) at 300 hPa between the two RASM-DPLE ensembles in Fig. S2.

Source	Sum of squares (SS)	Degree of freedom (df)	Mean squares (MS)	F-ratio	p-value
Between-groups variation (Column)	69963.1	1	69963.1	104.38	5.96e-20
Within-groups variation (Error)	132716.3	198	670.3		
Total	202679.4	199			

Table S2. The 3-hourly observed weather data (mean air temperature, mean wind direction, and mean wind speed) at Station 04312 (Station Nord) in February 2009. If any data are missing, they are not shown or indicated as (-).

Date	Time (local)	Air temperature (°C)	Mean wind direction (wind blowing from)	Mean wind speed ($m\ s^{-1}$)
6 February	0	–16.6	-	-
	3	–12.2	-	-
	6	–12.3	-	-
	9	–12.7	-	-
	12	–12.6	-	-
	15	–12.9	-	-
	18	–11.7	south-southwest	15
	21	–12.7	south-west	11
7 February	0	–13.0	south-southwest	16
	3	–13.1	south-west	14
	6	–13.0	south-west	15
	9	–12.6	south-west	16
	12	–13.7	south-southwest	19
	15	–18.0	west	4
	18	–17.2	west-northwest	2
	21	–13.6	south-west	11
8 February	0	–18.5	south-west	8
	3	–14.6	south-west	11
	6	–16.0	south-west	15
	9	–21.9	west	7
	12	–27.7	west-northwest	4
	15	–23.8	west	3
	18	–25.8	east-northeast	2
	21	–32.0	north-northwest	3
9 February	0	–32.4	south-west	5
	3	–33.5	south-west	4
	6	–31.0	south-west	3
	9	–29.8	south-west	3
10 February	3	–25.3	north-east	1
	6	–25.2	east	1
	9	–24.3	south-southwest	1
	12	–24.4	north-east	1
	15	–24.2	north	1
	18	–25.5	north-east	2
	21	–26.2	north	1
11 February	0	–28.5	south-west	2
	3	–29.6	south-west	4
12 February	6	–25.3	west-southwest	1
	9	–25.1	east-northeast	2
	12	–25.1	east	1
	15	–25.3	north-east	1
	18	–28.6	-	-
27 February	12	–29.5	south-west	2

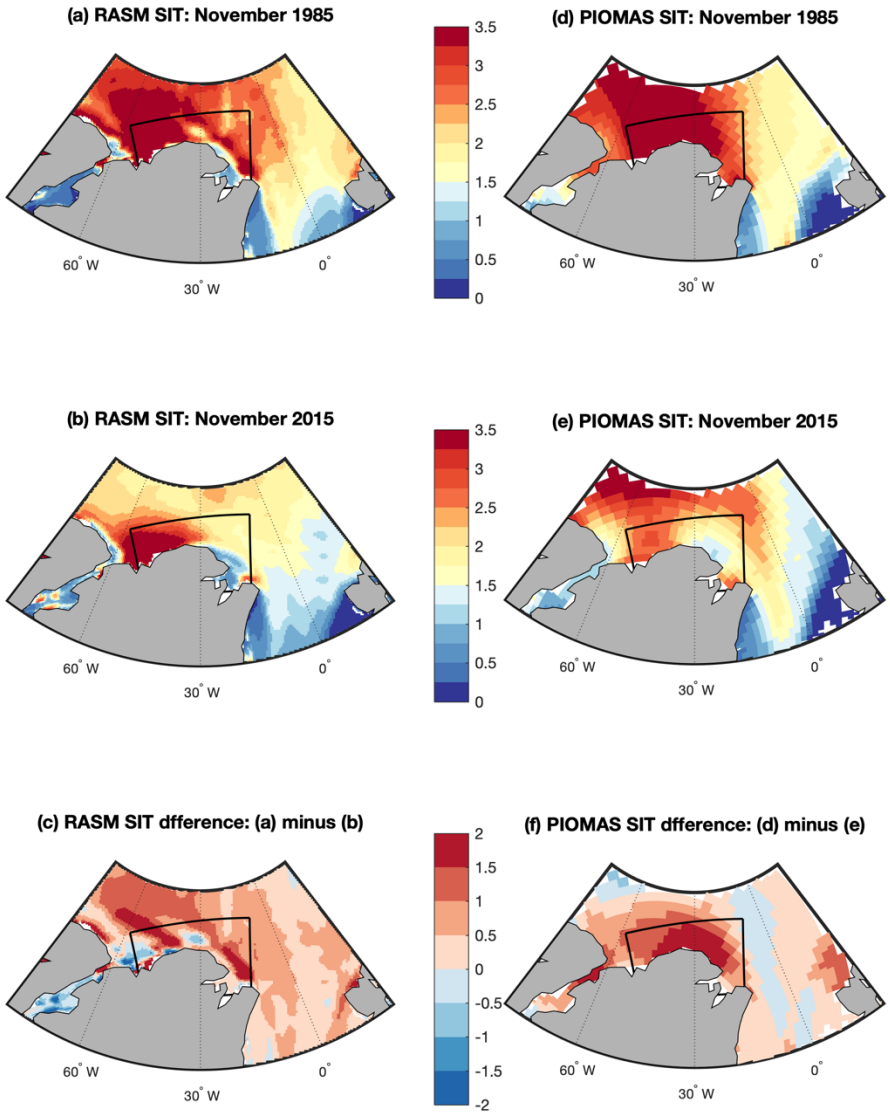

30

Figure S1. Monthly mean sea ice thickness (SIT; m) of the RASM hindcast in (a) November 1985, (b) November 2015, and (c) its difference between (a) and (b) over the polynya region (black line), and of PIOMAS in (d) November 1985, (e) November 2015, and (f) its difference between (d) and (e).

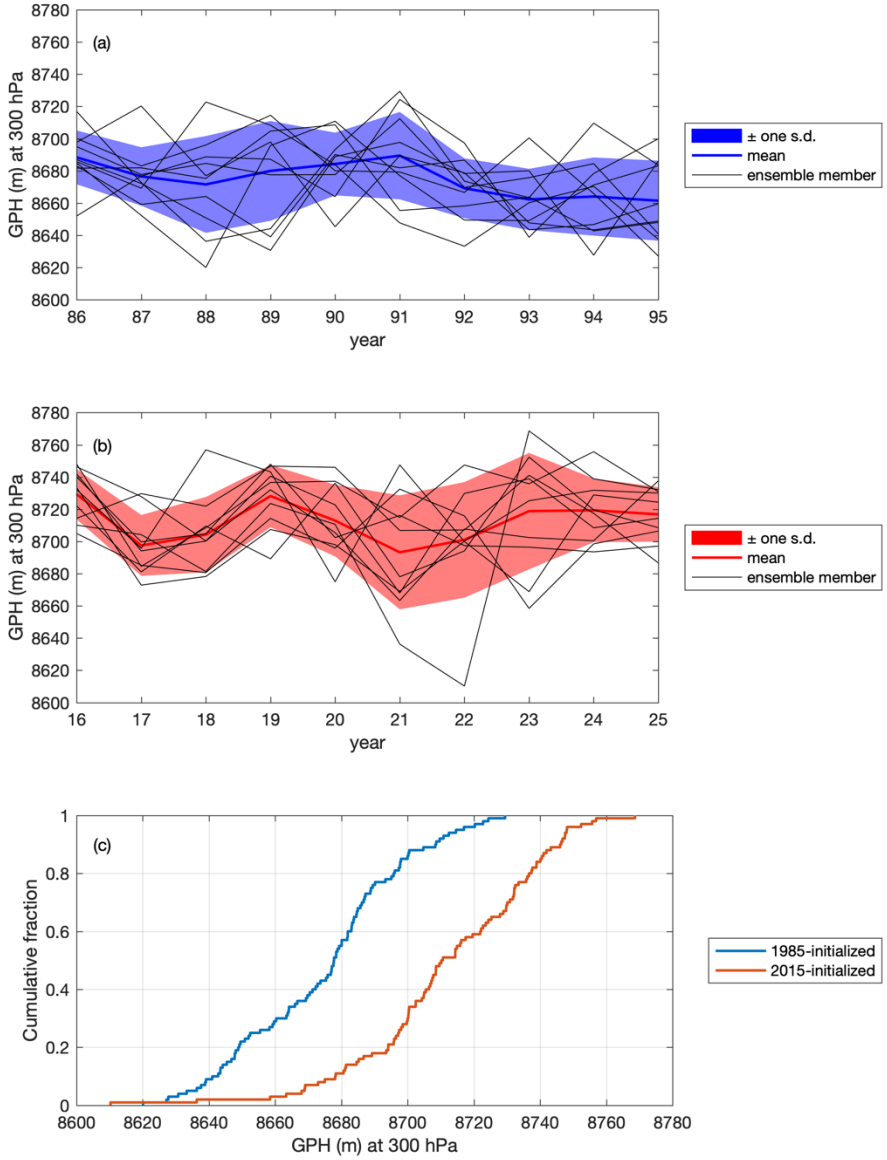

Figure S2. The annual mean of geopotential height (GPH; m) at 300 hPa in the central Arctic from the RASM-DPLE ensembles: (a) 1985-initialized and (b) 2015-initialized simulations. The black lines indicate 10 ensemble members. The blue and red solid lines are the ensemble mean with the shading of ± one standard deviation (s.d.) from the mean during 1986–1995 (blue) and 2016–2025 (red), respectively. (c) Cumulative distribution functions of GPH at 300 hPa are shown from the two RASM-DPLE ensembles above.

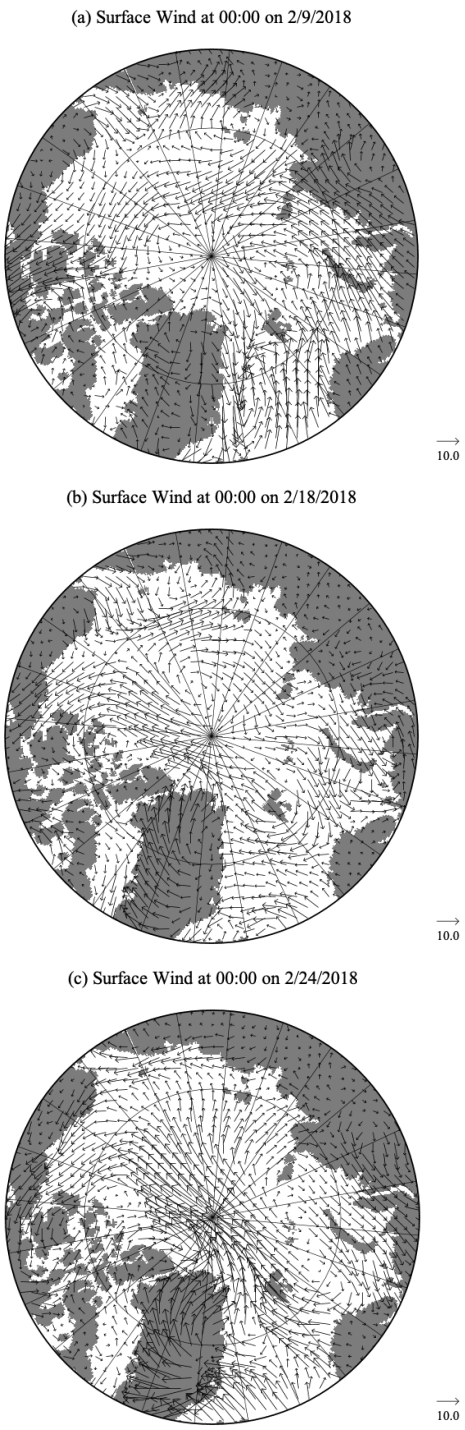

45

Figure S3. The 6-hourly near-surface (at 10 m) wind fields (m s^{-1}) from ERA-Interim atmospheric reanalysis at 00:00 on (a) 9 February 2018, (b) 18 February 2018, and (c) 24 February 2018

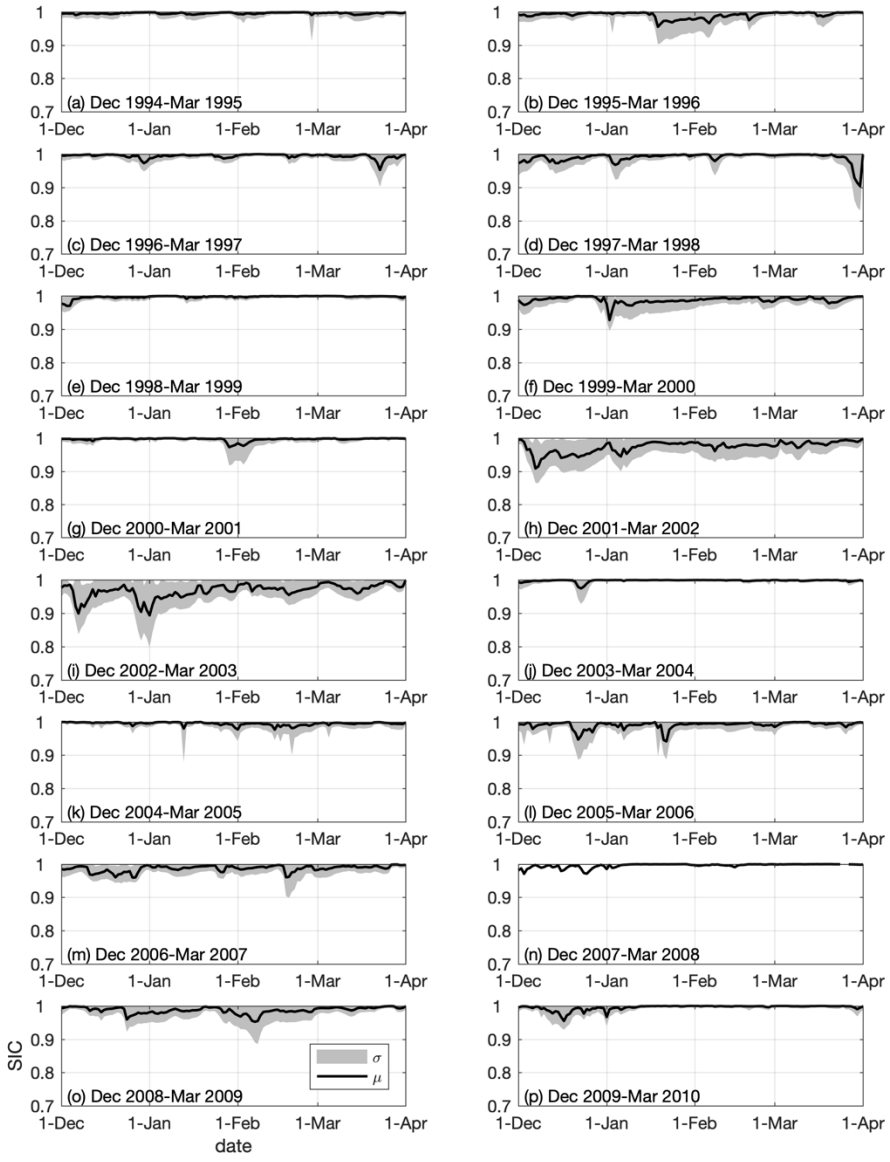

Figure S4. (a)-(p) Time series of satellite-derived (NASA Team algorithm) daily mean sea ice concentration (SIC; μ) (black) spatially averaged for the northern Greenland region (see Fig. 4a) on each day during winter months (December–March) from 1994 to 2010. The grey shading depicts one (spatial) standard deviation (σ) (gray) from the daily (spatial) mean SIC (μ).

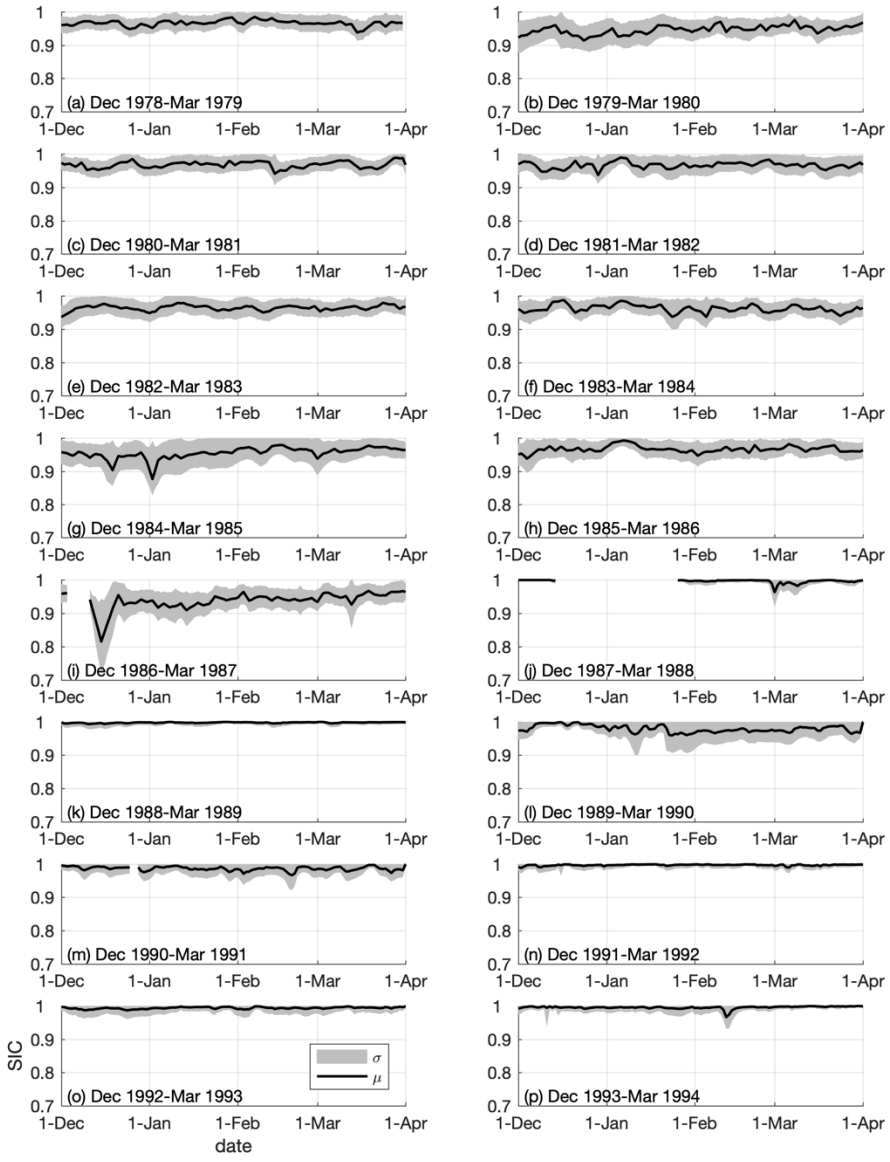

Figure S5. (a)-(p) Same as Fig. S3, but from 1978 to 1994. Note that data gaps are due to missing observations: i.e., December 1986 and 1987 as well as January 1987.

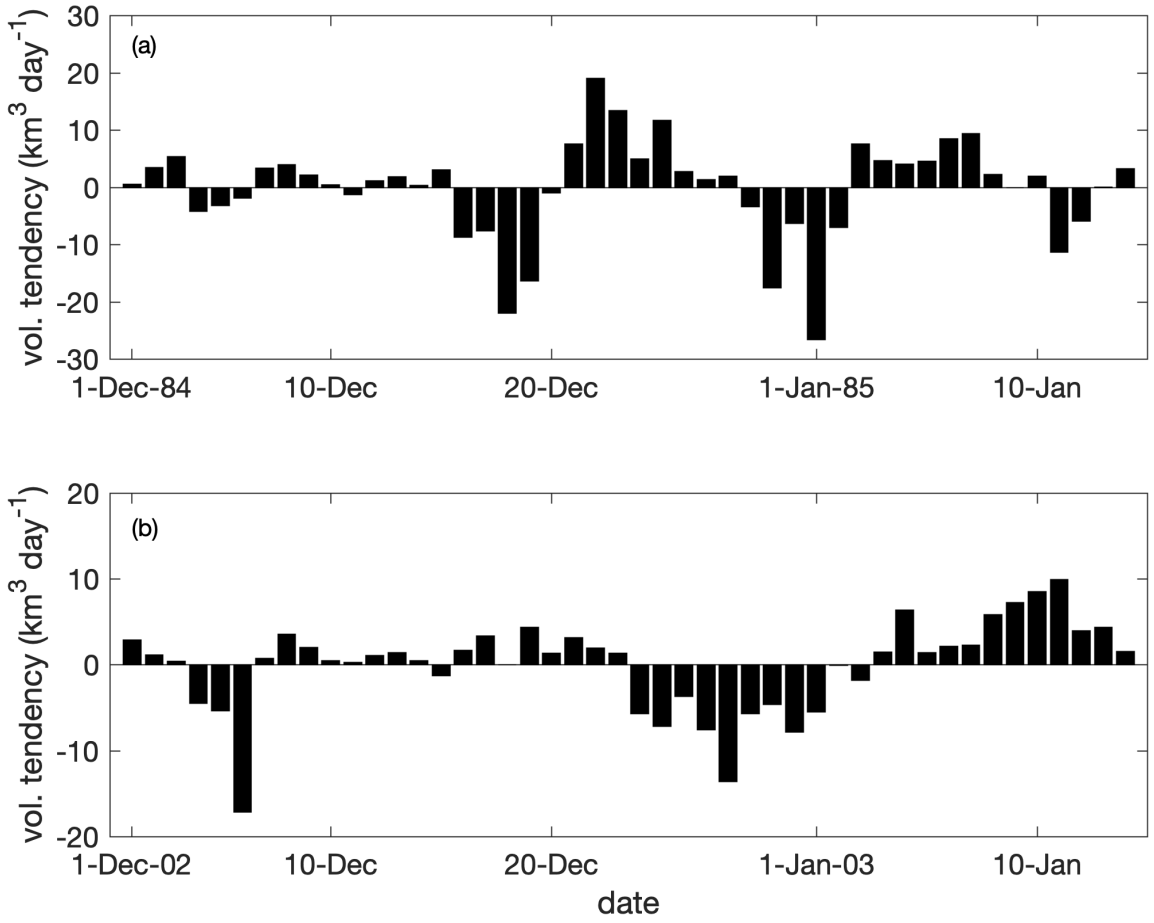

60

Figure S6. The time rate of change of the RASM daily sea ice volume (km^3 d^{-1}) due to dynamic tendency (a) during 1 December 1984–15 January 1985 and (b) during 1 December 2002–15 January 2003, spatially integrated for the region shown in Fig. 4(a).

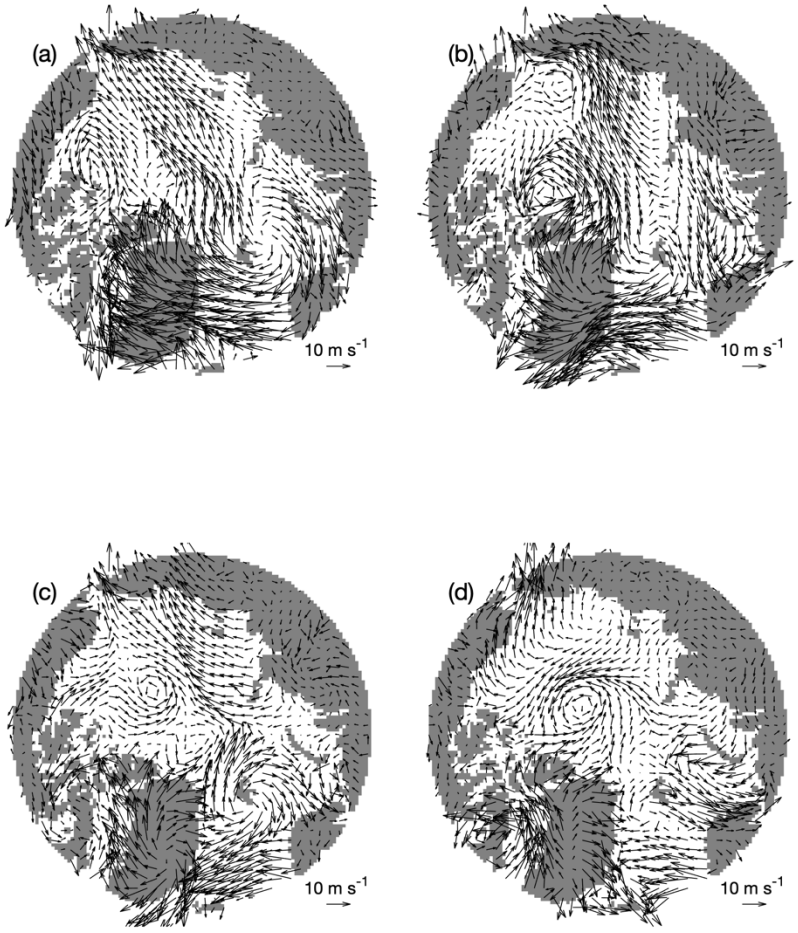

65

Figure S7. The near-surface (at 10 m) wind fields (m s^{-1}) from the RASM simulation at 00:00 on (a) 14 December 1986, (b) 16 December 1986, (c) 18 December 1986, and (d) 20 December 1986. The wind vectors were sub-sampled at every three grid cells for a plotting purpose.

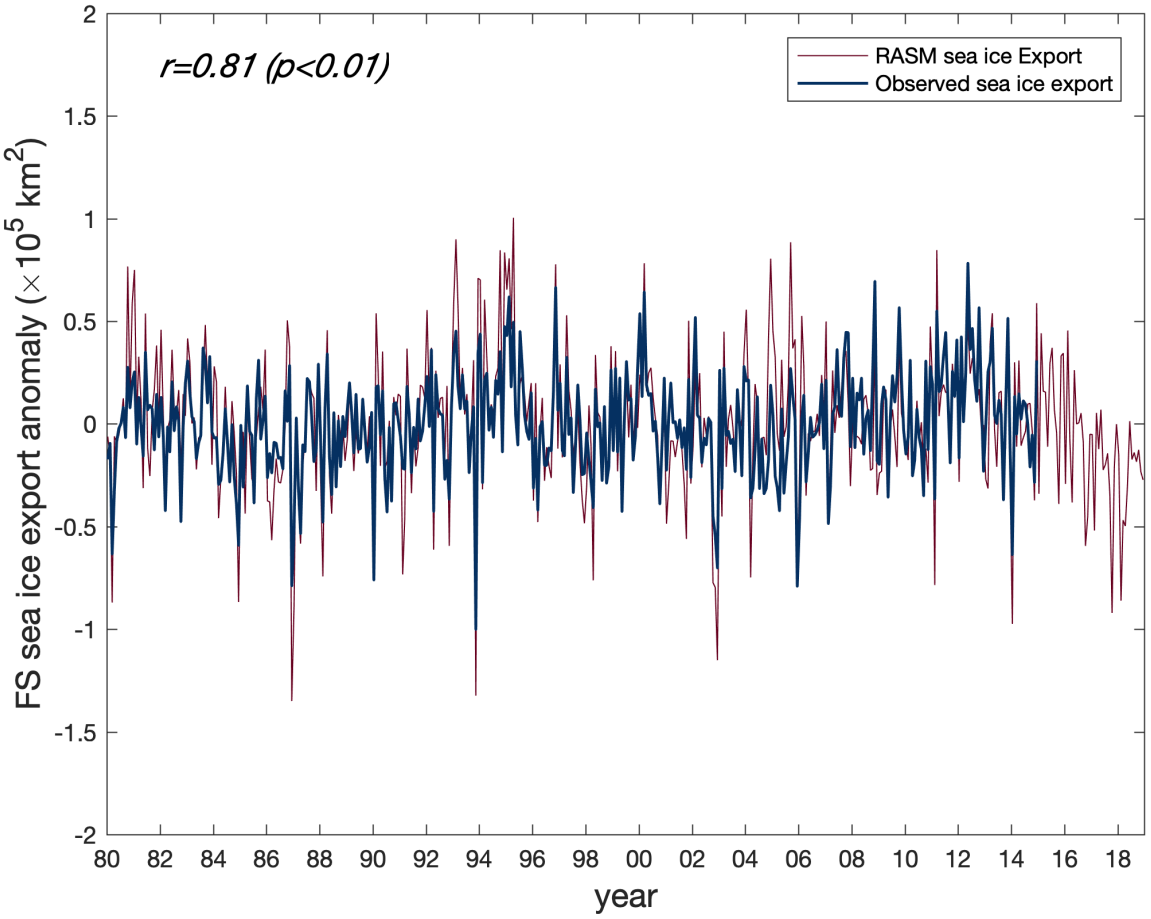

Figure S8. The monthly mean anomaly of Fram Strait (FS) sea ice export: the RASM simulation during 1980–2018 (red) and the observed data record during 1980–2014 (black) from https://doi.pangaea.de/10.1594/PANGAEA.868944. The correlation coefficient (*r*) between the RASM and observed ice export anomaly (1980–2014) is shown in the upper left.